Accepted Manuscript

Scale-up from batch to flow-through wet milling process for injectable depot formulation

Róbert Lehocký, Daniel Pěček, František Štěpánek

Scale-up from batch to flow-through wet milling process for injectable depot formulation

Róbert Lehocký[1,2], Daniel Pěček[2], František Štěpánek[1,*]

[1]Department of Chemical Engineering, University of Chemistry and Technology, Prague, Technická 5, 166 28 Prague 6, Czech Republic

[2]Zentiva, k.s., U Kabelovny 130, 102 00 Praha 10, Czech Republic

[*]Corresponding author. Tel.: +420 220 443 236; E-mail: Frantisek.Stepanek@vscht.cz

1

Abstract

Injectable depot formulations are aimed at providing long-term sustained release of a drug into systemic circulation, thus reducing plasma level fluctuations and improving patient compliance. The particle size distribution of the formulation in the form of suspension is a key parameter that controls the release rate. In this work, the process of wet stirred media milling (ball milling) of a poorly water-soluble substance has been investigated with two main aims: (i) to determine the parametric sensitivity of milling kinetics; and (ii) to develop scale-up methodology for process transfer from batch to flow-through arrangement. Ball milling experiments were performed in two types of ball mills, a batch mill with a 30 ml maximum working volume, and a flow-through mill with a 250 ml maximum working volume. Milling parameters were investigated in detail by methodologies of QbD to map the parametric space. Specifically, the effects of ball size, ball fill level, and rpm on the particle breakage kinetics were systematically investigated at both mills, with an additional parameter (flow-rate) in the case of the flow-through mill. The breakage rate was found to follow power-law kinetics with respect to dimensionless time, with an asymptotic d_{50} particle size in the range of 200-300 nm. In the case of the flow-through mill, the number of theoretical passes through the mill was found to be an important scale-up parameter.

1 Introduction

Intramuscular depot formulations are considered as a way of providing constant plasma levels of a drug over extended periods of time and improving patient compliance (Kisely et al., 2015; Wright et al., 2012). The principle of a depot formulation in the form of a suspension is based on the intramuscular injection (typically into *M. gluteus* or *M. deltoideus*) (Hough et al., 2009; Probst et al., 2016; Wright et al., 2012) of a poorly water-soluble drug, whereby the particles gradually dissolve and release the drug into systemic circulation. The release mechanism can be either a simple physical dissolution or reactive enzymatic dissolution (Owen, 2010; Yin et al., 2015).

For a given solid-state form of the drug, the depletion rate of the depot (and by consequence, the evolution of plasma concentration over time as well as the necessary renewal period of the depot, important for example in the case of contraceptives (Andrew and Kaunitz, 1994; Westhoff, 2003) depends on the specific surface area of the particles, and therefore on their size distribution and morphology (Leng et al., 2014). The particle size distribution is controlled by the manufacturing process. The required particle size distribution in depot formulations generally depends on the used API – its therapeutic dose, its solubility and the required treatment period. In our formulation the particle size d_{90} should be below 2.5 µm. A suspension of particles can in principle be formed either by a bottom-up approach from a solution (e.g. by precipitation (Du et al., 2015), solvent evaporation (Jallouli et al., 2015) or emulsion congealing (Hassan et al., 1995; Matos-Jr et al., 2015) or by a top-down approach from pre-existing solid particles (e.g. by wet milling (Afolabi et al., 2014; Li et al., 2015), high-pressure homogenisation (Möschwitzer, 2013; Tuomela et al., 2016) or their combination (Attari et al., 2016; Hatahet et al., 2016). Each approach has its advantages and disadvantages, related not only to the ability to control particle size distribution (mono- vs. poly-disperse), phase (amorphous vs. crystalline), and morphology (spherical vs. irregular), and but also to aspects such as technological complexity and industrial scalability. In the case of injectable suspensions, sterile production and the absence of solvent residues are particularly important factors to consider (Becker Peres et al., 2016; Wright et al., 2012).

The present work is concerned with the wet milling (stirred media milling) process, which belongs to the top-down category. The kinetics of stirred media wet milling has been extensively studied in the literature, especially in the context of the milling of inorganic materials such as metal oxides (Knieke et al., 2011). It was reported that the particle size follows power-law kinetics with respect to the integral energy input into the mill (Capece et al., 2013; Stenger et al., 2005), and that a certain asymptotic (or "irreducible") particle size is attained, which is controlled mainly by the electrostatic repulsion in the case of the inorganic nanoparticles and can therefore be influenced by the pH and ionic strength of the medium (Niwa et al., 2011). The wet milling of organic substances such as pharmaceuticals to sub-micrometer particle sizes has also been reported in several studies (Liu et al., 2011) ; similarly as in the case of inorganic particles, the power-law kinetics was found to hold. In the case of hydrophobic materials, the asymptotic particle size depends on the presence of a surfactant that stabilises the particle suspension (Shegokar and Müller, 2010). However, most studies that can be found in the literature deal with only one type or size of mill, and the practically important problem of parameter transfer between mills of different size, or from batch to continuous milling, has rarely been addressed.

Therefore, the aim of the present work was to propose a methodology for transferring the stirred media wet milling process from a batch to a flow-through (circulation) arrangement during process scale-up, and to demonstrate the methodology using an example of a pharmaceutically relevant formulation. In the spirit of the QbD (Quality by Design) methodology (Aksu et al., 2012; Loh et al., 2015; Rathore, 2016), a detailed mapping of the parametric space has been performed in order to identify the sensitivity of the milling kinetics (the time evolution of the particle size distribution) on the design and process parameters, and to use this knowledge for scale-up from batch to flow-trough process.

2 Materials and methods

2.1 Chemicals

The substance chosen for the development of the scale-up methodology was a hydrophobic API in the form of dry powder consisting of platelet-like crystals with a characteristic particle size between 5-300 μm. It has a low aqueous solubility (below 30 mg/l). The dispersion medium was a particle-free water for injections which meets pharmacopeia conditions, containing Tween 20 (Sigma-Aldrich, Czech Republic) and polyethylene glycol (PEG 4000, Sigma-Aldrich, Czech Republic) to stabilize the particles in suspension, as well as a buffering system (citric acid monohydrate at 0.5 % (w/w), sodium dihydrogen phosphate monohydrate at 0.2 % (w/w), disodium hydrogen phosphate anhydrous at 0.5 % (w/w), and sodium hydroxide at 0.3 % (w/w)) to adjust pH and ionic strength. The amount of the API in the suspension was fixed at 26.4 % (w/w) for the batch experiments and 15.6 % (w/w) for the flow-through experiments. The surfactant/API ratio was 0.076 for Tween 20 and 0.19 for PEG 4000. The viscosities of 3.0 % and 5.1 % aqueous solutions of PEG 4000 that were used in the experiments were 1.75 mPa.s and 1.86 mPa.s, respectively.

2.2 Ball milling process

The milling process was carried out in two types of stirred media mills (ball mills). At the smaller scale, the batch mill Picoliq (Hosokawa-Alpine, Germany) in batch mode using zirconium dioxide beads or various sizes (0.3, 0.4-0.6, or 0.8-1.0 mm in diameter) was used. The stirring speeds were 1000, 4000, or 7000 rpm and the ball fill ratio was 50 %, 75 %, or 100 % (corresponding to 8, 12, and 16 ml of the solid balls, respectively). According to the manufacturer, the recommended ball fill volume is 16 ml, which we further denote as a 100 % fill level. The total volume of the milling chamber was 30 ml and the real work volume depends on actual ball fill level. To follow the milling kinetics, samples were collected at predetermined time intervals and subjected to particle size distribution (PSD) analysis by static light scattering and morphology analysis by Scanning Electron Microscopy (SEM). In order to establish the reproducibility of the entire procedure, three independent realisations of the milling experiments were performed for the mid-point setting of the process parameters (4000 rpm, 75 % fill level, 0.4-0.6 mm ball size). The relative standard deviation of the mean particle size was 22.6 %.

At the larger scale, the milling was performed in an agitated bead mill Labstar (Netzsch, Germany) with a 250 ml milling chamber, operated in open or closed circulation mode using zirconium dioxide beads (0.5 or 1.0 mm in diameter) at stirring rates of 1000 or 3000 rpm and ball fill level of 50 % or 100 % (corresponding to 112.5 and 225 ml of the beads, respectively). Similarly as in the small-scale mill, the breakage kinetics was obtained by taking samples at pre-determined time intervals and measuring their PSD.

2.3 Particle characterization

2.3.1 Static light scattering

The particle size distribution (PSD) of the suspension was measured by static light scattering using the Malvern Mastersizer 2000 (Malvern Instruments, UK). The particle size distribution was volume-weighted and apart from the full PSD, the percentiles d_{10}, d_{50} and d_{90} were also evaluated. The particle size distribution measurements of the suspensions were performed diluted in a 230 ml flow cell, using deionized water as the dilution medium. Stirring and sonication was applied. The volume of the injected suspension into the flow cell was in the range of 30 to 250 µl, which was automatically indicated by the instrument. The PSD of the crude API suspension was measured in the same way (including all formulation components) as the milled suspensions.

2.3.2 Scanning Electron Microscopy

The morphology of the crude material as well as the milled, dried suspensions was observed by Scanning Electron Microscopy (Tescan, Czech Republic). A single drop of the suspension was placed on the SEM stub and dried at laboratory conditions for approximately one hour. Dry samples were sputter-coated by platinum and SEM micrographs taken in the high-vacuum mode using the back-scatter detector (BSE) at a typical acceleration voltage of 15 kV.

3 Results and discussion

3.1 Analysis of batch milling

The first set of experiments was carried out in the batch mill. The volume of the suspension containing 26.0 % of API was 14 ml, 18 ml or 22 ml depending on the ball fill level. The variable parameters were: ball size (0.3 mm, 0.4-0.6 mm or 0.8-1.0 mm), ball fill level (50 %, 75 % or 100 %), and stirring intensity (1000 rpm, 4000 rpm or 7000 rpm). For each set of parameters, the milling kinetics was followed by taking samples at fixed time intervals (3 min, 5 min, 10 min, 20 min, 30 min, 60 min, 120 min) and measuring the particle size distribution (PSD) by static light scattering. An example of the time evolution of the PSD is given in Fig. 1, and the SEM micrographs of the particles after different times of milling are shown in Fig. 2. It can be seen that the most significant size reduction occurs during the early stages of milling, whereby a majority of the batch drops below 10 µm within 3 minutes, achieving a reduction in the d_{50} particle diameter by a factor of 10 compared to the raw

material. The particle morphology also changes significantly, from platelet-like crystals of the starting material to rounded particles with aspect ratio closer to one, as the milling progresses.

From the obtained experimental data for all parameter combinations, the 10, 50 and 90-percentile particle diameters (d_{10}, d_{50}, and d_{90}) were evaluated from the volume-based size distributions and plotted as a function of time. As an indication of the effectiveness and parametric sensitivity of the milling process, the times required for d_{50} to fall below 1 µm under various parameter combinations are summarised in Table 1. The most effective milling conditions were found to be at 7000 rpm, 100 % ball fill level, 0.3 mm ball size. These have lead to the shortest required milling times because of the highest number of effective collision events, while milder conditions (1000 rpm, 50 % fill level, larger balls) resulted in slower milling. The important finding is that the particle population can be reduced below a given target size by a number of different parameter combinations, but the time required to do so varies widely, from less than 1 min for the most effective milling conditions, to well over 120 min for the mildest ones.

Table 1: Time required for the particle size d_{50} to fall below 1 μm.

Milling conditions	Ball diameter (mm)	0.3	0.3	0.3	0.3	0.8-1.0	0.8-1.0	0.8-1.0	0.8-1.0
	Stirring speed (rpm)	1000	1000	7000	7000	1000	1000	7000	7000
	Ball fill level (%)	50	100	50	100	50	100	50	100
Time (min)		>120	107	8.5	<1	>120	>120	40	14

In order to compare the milling kinetics for different parameter combinations, the particle size was plotted as function of dimensionless time, which reflects the number of "effective collision events" that occurred in the mill, defined as

$$N_{eff} = time \times rpm \times (ball\ fill\ level)^2 \tag{1}$$

The rationale behind this definition is that in stirred media mills, the particle breakage is assumed to occur predominantly at the contact points between a pair of colliding balls. For a given volume of the mill chamber and size of the balls, the number of collision events per unit of time is proportional to the square of the number of balls in the mill and to the stirring intensity. The absolute number of collision events is then proportional to the product of rpm and time. The second-order kinetics (i.e. proportionality to the square of the number of milling beads) was tested against a first-order kinetics and found to agree better with the experimental data. This is consistent with a milling mechanism based on binary collisions between pairs of balls, rather than, e.g. individual particle-ball collisions or friction.

The particle size d_{50} as function of the dimensionless time is summarised in Fig. 3 for eight parameter combinations, grouped by the ball size. Note that in the case of the larger ball size (0.8-1.0 mm) shown in Fig. 3a, all four parameter combinations follow very similar power-law breakage kinetics with a scaling exponent in a relatively narrow range between -0.755 and -0.581 when using the dimensionless time as the independent variable. Such "universal" breakage kinetics then enables accurate estimation of the required milling time for different choices of ball fill level and rpm of the mill, which may be required during formulation development for various reasons such as foam control, avoiding overheating, etc. However, it has to be kept in mind that the exact numerical value of the scaling exponent is of course

specific to the materials (API molecule and suspension composition) for which it has been measured.

In the case of the smaller ball size (0.3 mm, shown in Fig. 3b), the breakage kinetics also appears to follow a power law dependence of particle size on the dimensionless time, but there is now a much wider range of scaling exponents and it appears that the process goes through three characteristic stages: (i) an initial "induction" stage without strong variation of particle size; (ii) the actual "milling" stage that follows power-law kinetics with a steeper slope, and (iii) a final stage where the particle size seems to have reached an asymptotic value, sometimes called the "irreducible particle size". The initial induction period can be explained by the need for a certain fatigue to accumulate in the particles before they begin to break, possibly due the smaller kinetic energy of the 0.3 mm balls compared to the 0.8-1.0 mm balls under otherwise identical conditions. Assuming similar collision velocities, the kinetic energy of the impact is smaller by a factor of approx. 27 in the case of the smaller balls, which could mean that the breakage at 1000 rpm does not start immediately and repeated impacts are needed before the particles start to fail. On the other hand, the absolute number of collision events per unit volume is higher in the case of the 0.3 mm balls due the larger number of balls (approx. 665 750 of 0.3 mm balls vs. 22 980 of 0.8-1.0 mm balls at 100 % fill), which can explain that for the harsher conditions (7000 rpm), the irreducible particle size was reached within the time frame of the experiment while it was not yet reached in the case of the larger balls under otherwise identical conditions.

All three stages of the milling process did not appear for all parameter combinations. In the case of experiments performed at 7000 rpm we did not catch the initial induction stage probably because this stage has occurred before the first sample was withdrawn at 3 minutes time. On the other hand, in the case of experiments performed at 1000 rpm the final stage of irreducible particles has not been reached because the process lasted only 120 minutes, which was not enough to reach the final stage at these milder milling conditions. Note that the regression lines in Fig. 3 are based on sub-sets of the experimental data points that belong to each characteristic stage. In order to confirm that even "mild" milling conditions can cover all three stages, the case of 1000 rpm, 50 % fill level, 0.3 mm balls was repeated with a starting material that was pre-milled to approx 10 μm. This experiment is shown in Fig. 3c and compared with data for identical conditions but starting from the original crude API. The absolute duration of each experiment is the same, i.e. 120 min. As can be seen, the pre-milled

material goes directly into the "milling" stage without any induction period, and reaches the asymptotic stage.

3.2 Breakage kinetics in a continuous mill

Having characterised the breakage process in a batch mill with a maximum working volume of 30 ml of suspension, the next step of the process scale-up was a flow-through mill with a maximum 250 ml working volume and a recirculation vessel of up to 2 000 ml storage capacity. Although the flow-through mill works on the same principle as the batch counterpart – i.e., wet stirred media milling – there is not automatically a direct equivalence between the two mills in terms of parameter transfer. In addition to the conditions in the actual milling chamber, which can be controlled by the combination of ball size, ball fill level, and stirring intensity (rpm), two additional parameters that can influence the milling kinetics in the flow-through mill are the recirculation flow-rate, which determines the mean residence time of the suspension in the milling chamber during a single pass ($\tau = V_{work} / Q_{circ}$), and the ratio of the mill working volume to the total suspension volume, which determines the volume fraction of the suspension that is being milled at any given moment, defined as $f_V = V_{work} / V_{tot}$. In our specific case, the flow-rate was varied from $Q_{circ} = 112.6$ ml/min to $Q_{circ} = 503$ ml/min (giving a mean residence time in the milling chamber between $\tau = 12.6$ s and $\tau = 94.8$ s depending on the ball fill level). The second parameter varied between $f_V = 0.33$ and $f_V = 0.56$ ($V_{work} = 106\text{-}178$ ml depending on the ball fill level, $V_{tot} = 320$ ml was constant).

The flow-through mill can be operated in two regimes: open loop and closed loop. The open loop mode provides information about the extent of particle breakage upon a single pass through the milling chamber, whereas the closed loop mode is similar to a batch process, except that only a certain fraction of the batch (f_V) is exposed to the milling conditions at any given moment. An example of particle size distributions collected from the outlet stream at different times during a single pass through the mill in the open loop mode is shown in Fig. 4 for 1000 rpm, 100 % fill level, 1.0 mm balls and 112.6 ml/min flow-rate and compared with the PSD of the feed raw material. It can be seen that even a single pass through the mill under these conditions is quite effective, resulting in all particles falling below 10 µm and a small population of sub-micron particles being formed as well. In theory, the PSD in the outlet stream in the open loop mode should be constant in time if the feed composition is constant. As can be seen in Fig. 4, up to a few minor fluctuations, this condition is met.

When the mill was operated in the closed loop mode, the particle size distribution as function time was processed in the same way as for the batch mill, and plotted in the form of d_{50} as function of dimensionless time. The results are summarised in Fig. 5a for a ball size of 1 mm and Fig. 5b for a ball size of 0.5 mm. In both cases, several combinations of stirring rate (1000 and 3000 rpm), ball fill level (50 % and 100 %) and circulation flow rate (112.6 and 503 ml/min) were compared, and it can be seen that despite the wide range of experimental conditions, power-law breakage kinetics with scaling exponents in the range from −0.896 to -1.427 for 0.5 mm balls and from −0.714 to −0.884 for 1.0 mm balls fit the experimental data very well, as in the case of the batch mill (cf. Fig. 3).

3.3 Scale-up considerations

However, when considering the time evolution of the particle size distributions in detail, there is an important difference between the batch and the flow-through mill. Due to the fact that the recirculation vessel contains both the feed suspension and the return from the milling chamber, it can be expected that a mixed population of particles with different processing history will develop over time and at any given moment, the suspension will contain particles that have been circulated through the mill a different number of times. It follows from the open loop experiments that a multi-modal PSD can temporarily develop in the suspension if the fine particles from the outlet stream after the first pass are returned to the recirculation vessel and mixed with the un-milled raw material. The theoretical number of passes of the entire batch through the mill can be estimated as

$$N = time \times Q_{circ} / V_{tot} \tag{2}$$

where Q_{circ} is the volumetric flow-rate through the mill and V_{tot} is the total volume of the suspension. Typically, V_{tot} would be the scale-up parameter of the process, as it depends on the required volume of the suspension that should be manufactured. It can be expected that for low values of N the PSD should be multi-modal, while for larger values of N, only the fine breakage products should prevail and the PSD should become monomodal. In the asymptotic limit of long times, all particles should converge to the "irreducible" particle size regardless of how many times they have been through the mill.

To verify this hypothesis, the particle size distribution as function of time was analysed in detail. Fig. 6a shows an example of the PSD evolution for one selected set of process parameters, namely 1000 rpm, 0.5 mm balls, 100 % fill level, and 503 ml/min recirculation flowrate. As can be seen, the PSD is indeed bi-modal for a period of time, but the mode corresponding to the larger particles gradually disappears as time progresses. The co-existence of particles that have already been circulated through the mill and those that have not, is clearly apparent also from the SEM micrographs taken at different times (Fig. 7). The bi-modal character of the PSD was observed also for other milling parameters, but the rate of disappearance of the upper mode from the PSD was different, and found to depend mainly on the recirculation rate. Examples of PSD evolution at a lower circulation flow-rate (112.6 ml/min) but otherwise similar conditions in the milling chamber as in the case from Fig. 6a (1000 rpm, 100 % fill level) are shown in Fig. 6b (0.5 mm balls) and Fig. 6c (1.0 mm balls), respectively.

When the particle size d_{50} is plotted as function of the theoretical number of passes, defined by Eq. 2, all the investigated cases follow similar trend-lines, with power law exponents ranging from -1.427 to -0.714 (Fig. 8). Thus, for the scale-up of the flow-through milling process, it is important to consider not only the conditions in the milling chamber, but also the exposure of the entire suspension to those conditions, which is expressed by the number of theoretical passes, *N*.

4 Conclusions

The formation of a particle suspension by wet milling in two types and scales of ball mills – a 30 ml batch mill and a 250 ml flow-through mill – has been investigated. The parametric dependence of the particle breakage kinetics on the main process parameters, namely ball size, ball fill level, stirring rate and (in the case of the flow-through mill) recirculation flow rate, has been systematically investigated and found to follow power-law kinetics with respect to a dimensionless time, defined as the relative number of ball collision events experienced by the particle suspension. While the exact numerical values of the kinetic parameters are of course specific for the investigated formulation, the methodology and the obtained trends could be generalised also to other systems. The same terminal particle size can thus in principle be obtained by several different combinations of ball fill level, stirring rate and overall process time, providing a degree of process flexibility to include additional factors

such as ball attrition or heat dissipation. As an example, let as consider the target of the particle size to be less than 2.5 μm as specified in the Introduction section. In a batch mill, a d_{50} of 2.17 μm can be achieved by the combination of 1000 rpm, 0.3 mm ball size and 100 % fill level in a milling time of 60 min. An almost identical particle size ($d_{50} = 2.11$ μm) has been reached in a flow-through milling process at 3000 rpm, 1.0 mm bead size, 50 % fill level and a recirculation rate of 112.6 ml/min in 10 min. Thus, both milling processes (batch and flow-through) are able to generate particles suitable for injectable depot formulations. Moreover, even significantly smaller particles in the sub-micron range can be achieved if desired.

In the case of the flow-through mill, the concept of effective collision events was found to hold as well, but the evolution of the particle size distribution was qualitatively different, going through a period of bi-modal PSD due to a distribution of processing history for individual particles within the batch, which was characterised by the number of theoretical passes through the mill (product of time and volumetric flow-rate over the entire batch volume). For sufficiently large number of passes, the PSD became narrower and the same terminal particle size as in the batch case has been achieved. Thus, the combination of the process conditions in the milling chamber, which has been parametrised in the form of a power-law function, and the number of passes in the case of a flow-through mill, together define the efficiency of the milling process and enable its rational scale-up.

Acknowledgments

References

Afolabi, A., Akinlabi, O., Bilgili, E., 2014. Impact of process parameters on the breakage kinetics of poorly water-soluble drugs during wet stirred media milling: A microhydrodynamic view. European Journal of Pharmaceutical Sciences 51, 75-86.

Aksu, B., Beer, T.D., Folestad, S., Ketolainen, J., Lindén, H., Lopes, J.A., Matas, M.D., Oostra, W., Rantanen, J., Weimer, M., 2012. Strategic funding priorities in the pharmaceutical sciences allied to Quality by Design (QbD) and Process Analytical Technology (PAT). European Journal of Pharmaceutical Sciences 47, 402-405.

Andrew, M., Kaunitz, M.D., 1994. Long-acting injectable contraception with depot medroxyprogesterone acetate. American Journal of Obstetrics and Gynecology 170, 1543-1549.

Attari, Z., Bhandari, A., Jagadish, P.C., Lewis, S., 2016. Enhanced ex vivo intestinal absorption of olmesartan medoxomil nanosuspension: Preparation by combinative technology. Saudi Pharmaceutical Journal 24, 57-63.

Becker Peres, L., de Araújo, P.H.H., Sayer, C., 2016. Solid lipid nanoparticles for encapsulation of hydrophilic drugs by an organic solvent free double emulsion technique. Colloids and Surfaces B: Biointerfaces 140, 317-323.

Capece, M., Dave, R., Bilgili, E., 2013. Influence of non-linear breakage kinetics on the attainment of self-similarity for dry milling processes. Chemical Engineering Science 97, 96-107.

Du, J., Li, X., Zhao, H., Zhou, Y., Wang, L., Tian, S., Wang, Y., 2015. Nanosuspensions of poorly water-soluble drugs prepared by bottom-up technologies. International Journal of Pharmaceutics 495, 738-749.

Hassan, E.E., Eshra, A.G., Nada, A.H., 1995. Formulation of prolonged release lipid micropellets by emulsion congealing: Optimization of ketoprofen entrapment and release. International Journal of Pharmaceutics 121, 149-155.

Hatahet, T., Morille, M., Hommoss, A., Dorandeu, C., Müller, R.H., Bégu, S., 2016. Dermal quercetin smartCrystals®: Formulation development, antioxidant activity and cellular safety. European Journal of Pharmaceutics and Biopharmaceutics 102, 51-63.

Hough, D., Lindenmayer, J.-P., Gopal, S., Melkote, R., Lim, P., Herben, V., Yuen, E., Eerdekens, M., 2009. Safety and tolerability of deltoid and gluteal injections of paliperidone palmitate in schizophrenia. Progress in Neuro-Psychopharmacology and Biological Psychiatry 33, 1022-1031.

Jallouli, Y., Willart, J.F., Siepmann, F., Descamps, M., Danede, F., Siepmann, J., 2015. Preparation of polymeric fenofibrate formulations with accelerated drug release: Solvent evaporation versus co-grinding. Journal of Drug Delivery Science and Technology 30, Part B, 397-407.

Kisely, S., Sawyer, E., Robinson, G., Siskind, D., 2015. A systematic review and meta-analysis of the effect of depot antipsychotic frequency on compliance and outcome. Schizophrenia Research 166, 178-186.

Knieke, C., Romeis, S., Peukert, W., 2011. Influence of process parameters on breakage kinetics and grinding limit at the nanoscale. AIChE Journal 57, 1751-1758.

Leng, D., Chen, H., Li, G., Guo, M., Zhu, Z., Xu, L., Wang, Y., 2014. Development and comparison of intramuscularly long-acting paliperidone palmitate nanosuspensions with different particle size. International Journal of Pharmaceutics 472, 380-385.

Li, M., Yaragudi, N., Afolabi, A., Dave, R., Bilgili, E., 2015. Sub-100 nm drug particle suspensions prepared via wet milling with low bead contamination through novel process intensification. Chemical Engineering Science 130, 207-220.

Liu, P., Rong, X., Laru, J., van Veen, B., Kiesvaara, J., Hirvonen, J., Laaksonen, T., Peltonen, L., 2011. Nanosuspensions of poorly soluble drugs: Preparation and development by wet milling. International Journal of Pharmaceutics 411, 215-222.

Loh, Z.H., Samanta, A.K., Sia Heng, P.W., 2015. Overview of milling techniques for improving the solubility of poorly water-soluble drugs. Asian Journal of Pharmaceutical Sciences 10, 255-274.

Matos-Jr, F.E., Di Sabatino, M., Passerini, N., Favaro-Trindade, C.S., Albertini, B., 2015. Development and characterization of solid lipid microparticles loaded with ascorbic acid and produced by spray congealing. Food Research International 67, 52-59.

Möschwitzer, J.P., 2013. Drug nanocrystals in the commercial pharmaceutical development process. International Journal of Pharmaceutics 453, 142-156.

Niwa, T., Miura, S., Danjo, K., 2011. Universal wet-milling technique to prepare oral nanosuspension focused on discovery and preclinical animal studies – Development of particle design method. International Journal of Pharmaceutics 405, 218-227.

Owen, R.T., 2010. Paliperidone palmitate injection: Its efficacy, safety and tolerability in schizophrenia. Drugs Today (Barc) 46, 463-471.

Probst, M., Kühn, J.-P., Scheuch, E., Seidlitz, A., Hadlich, S., Evert, K., Oswald, S., Siegmund, W., Weitschies, W., 2016. Simultaneous magnetic resonance imaging and pharmacokinetic analysis of intramuscular depots. Journal of Controlled Release 227, 1-12.

Rathore, A.S., Quality by Design (QbD)-Based Process Development for Purification of a Biotherapeutic. Trends in Biotechnology 34, 358-370.

Shegokar, R., Müller, R.H., 2010. Nanocrystals: Industrially feasible multifunctional formulation technology for poorly soluble actives. International Journal of Pharmaceutics 399, 129-139.

Stenger, F., Mende, S., Schwedes, J., Peukert, W., 2005. Nanomilling in stirred media mills. Chemical Engineering Science 60, 4557-4565.

Tuomela, A., Saarinen, J., Strachan, C.J., Hirvonen, J., Peltonen, L., 2016. Production, applications and in vivo fate of drug nanocrystals. Journal of Drug Delivery Science and Technology 34, 21-31.

Westhoff, C., 2003. Depot-medroxyprogesterone acetate injection (Depo-Provera®): a highly effective contraceptive option with proven long-term safety. Contraception 68, 75-87.

Wright, J.C., Burgess, D.J., 2012. Long Acting Injections and Implants. Springer, Boston, MA.

Yin, J., Collier, A.C., Barr, A.M., Honer, W.G., Procyshyn, R.M., 2015. Paliperidone Palmitate Long-Acting Injectable Given Intramuscularly in the Deltoid Versus the Gluteal Muscle Are They Therapeutically Equivalent? Journal of Clinical Psychopharmacology 35, 447-449.

Figures
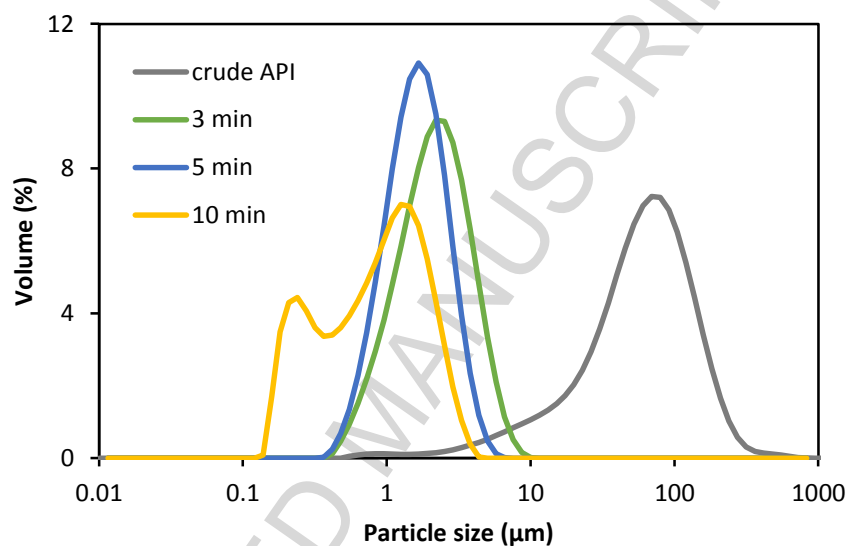
Fig. 1: Example of the evolution of particle size distribution measured by static light scattering during batch wet milling process (milling conditions: 7000 rpm, ball size 0.3 mm, ball fill level 50 %).
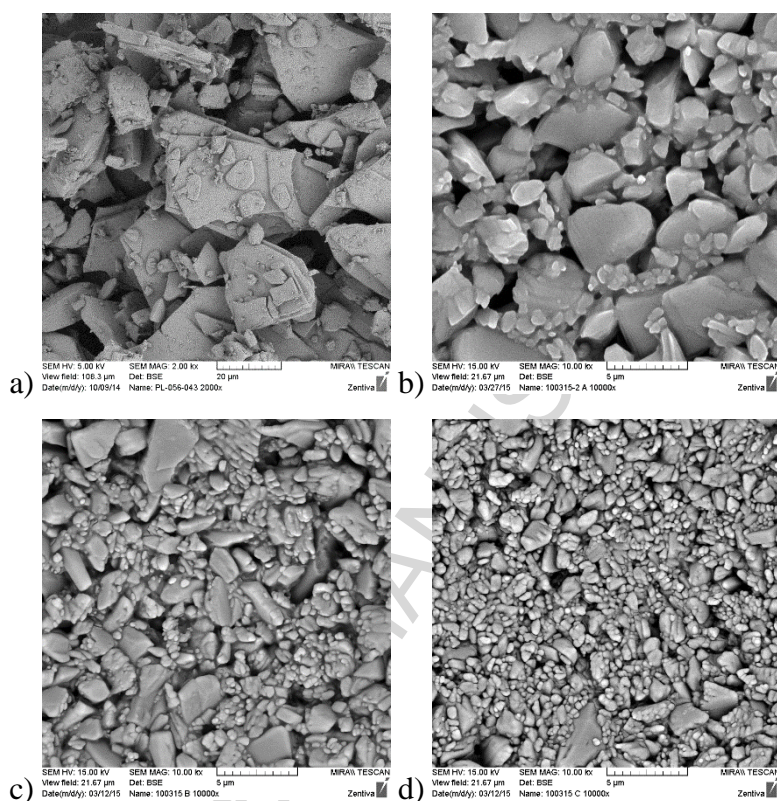
Fig. 2: SEM micrographs showing the evolution of particle morphology during batch wet milling. a) starting raw material; b) milling after t = 3 min; c) t = 5 min; d) t = 10 min. Milling conditions: 4000 rpm, ball size 0.4–0.6 mm, ball fill level 75%. Note that the scale-bar represents 50 µm for the raw material and 5 µm for the remaining cases.
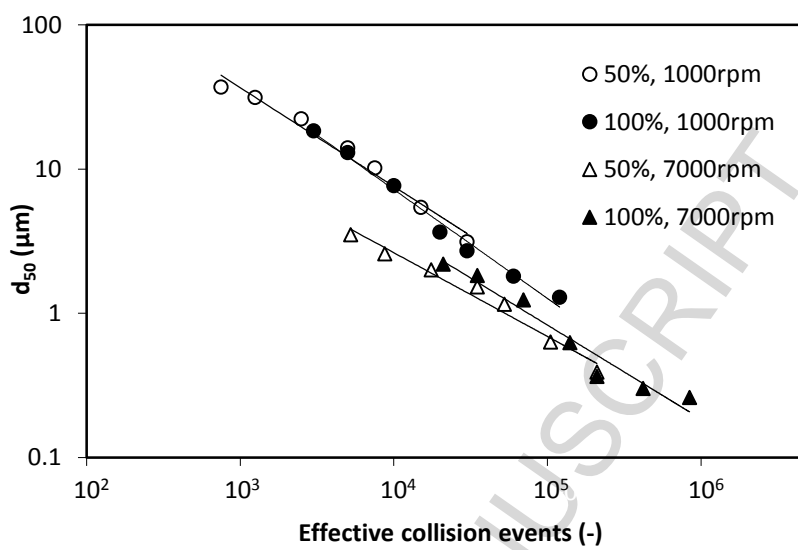
a)
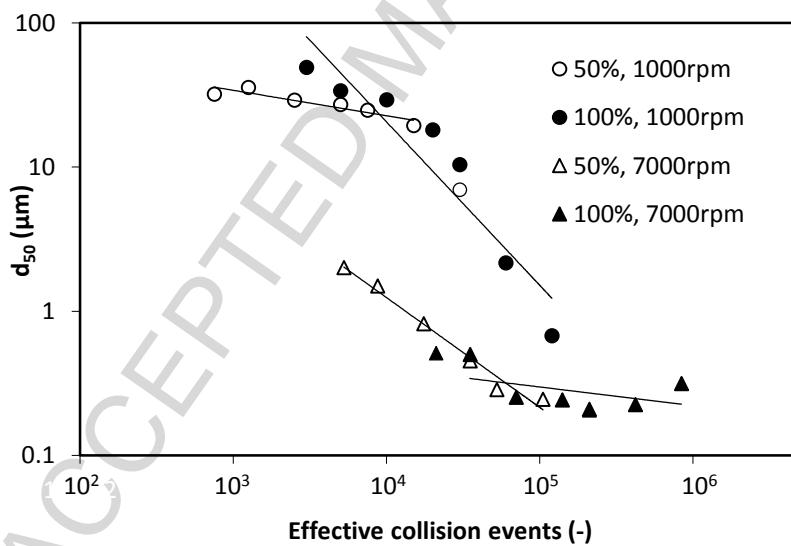
b)
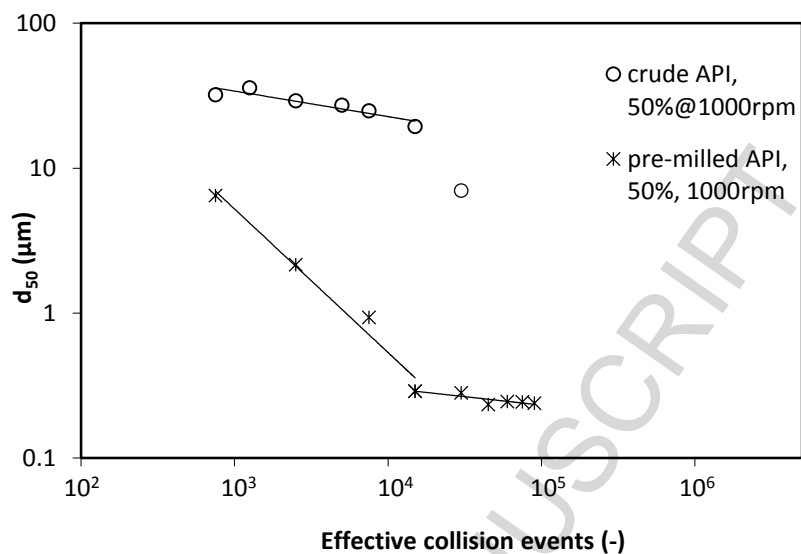
c)

Fig. 3: Evolution of the particle size d_{50} measured by static light scattering during batch milling process. a) Ball size 0.8-1.0 mm; b) ball size 0.3 mm; c) identical conditions as in case b), starting either from the original crude API or from a pre-milled API. The values of rpm and ball fill level are given in the legend. The lines represent regression fits by a power-law function.
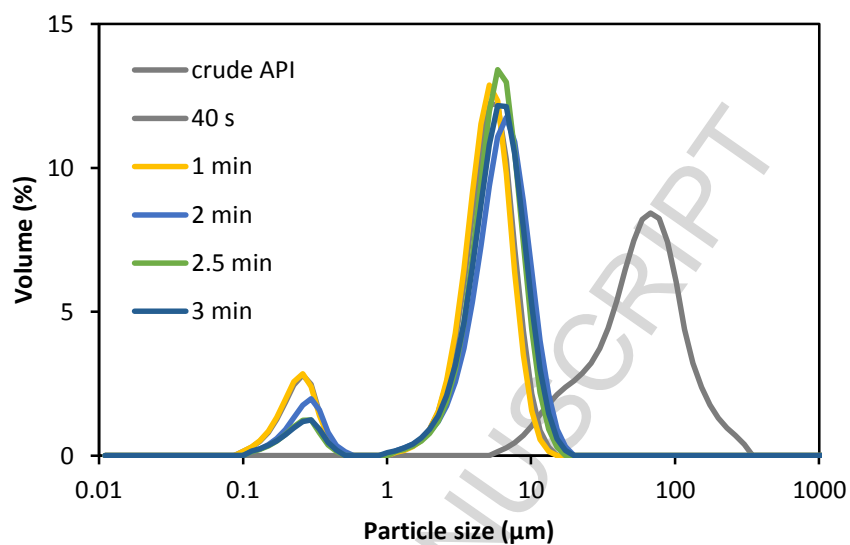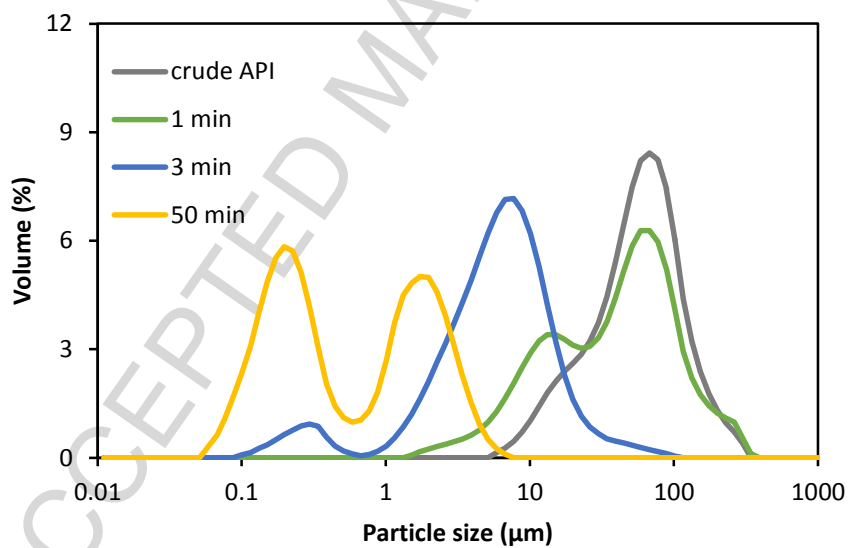
Fig. 4: Particle size distribution in the outlet from the milling chamber at different times during open loop continuous milling. The milling conditions were 1000 rpm, ball size 1.0 mm, ball fill level 100%, 112.6 ml/min flow rate (residence time in the mill 12.6 s).
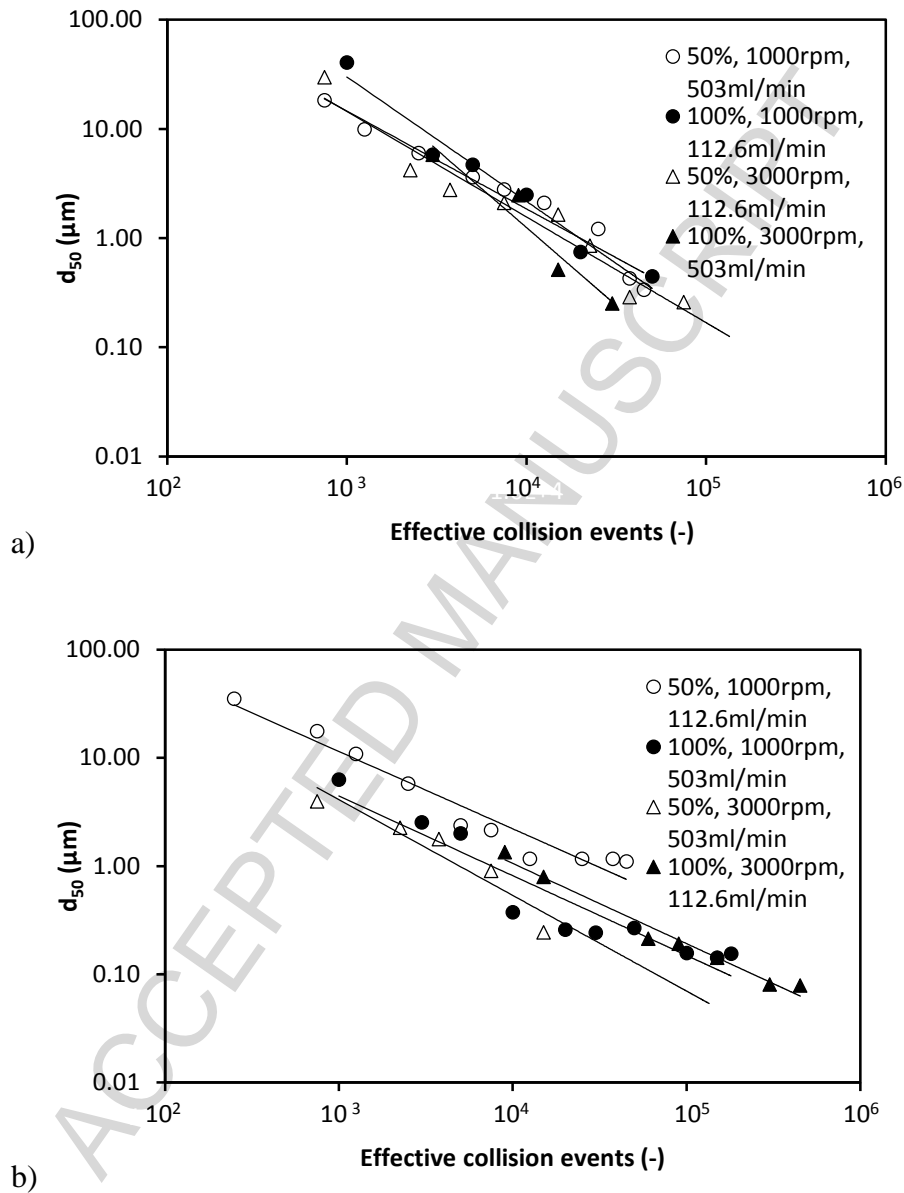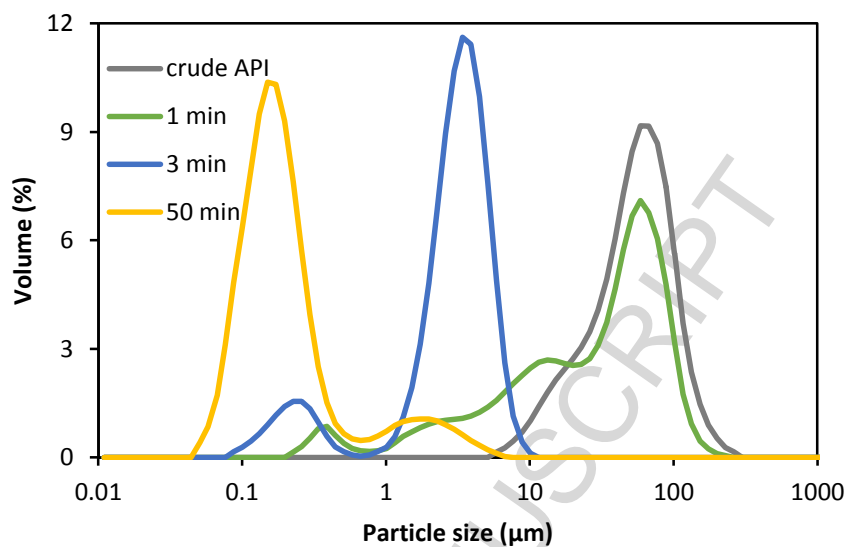
Fig. 5: Evolution of the particle size d_{50} during close loop milling process for conditions indicated in the legend. a) Ball size 1.0 mm; b) ball size 0.5 mm. The lines are regression fits by a power-law function.
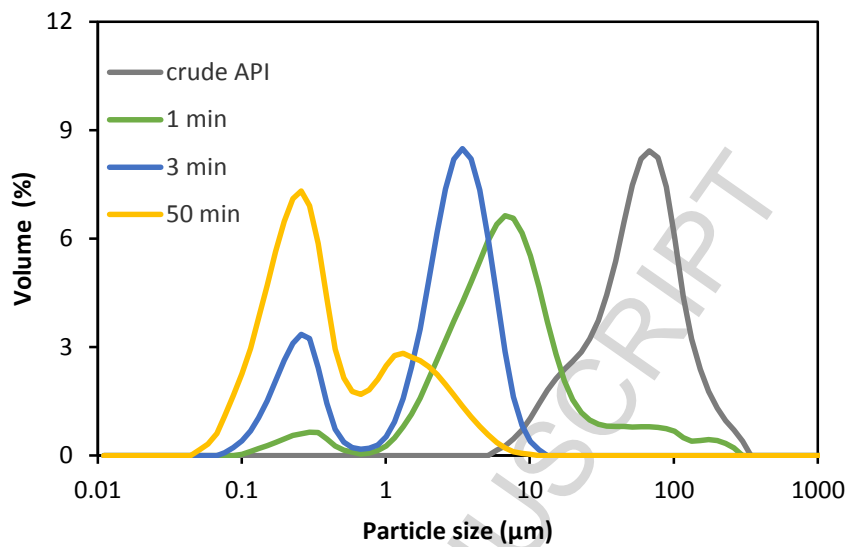
a)

b)

c)

Fig. 6: Evolution of the particle size distribution during flow-through milling in the closed loop mode. a) Milling conditions: 1000 rpm, ball size 0.5 mm, ball fill level 100%, recirculation flow-rate 503 ml/min. b) Milling conditions: 1000 rpm, ball size 1.0 mm, ball fill level 100%, recirculation flow-rate 112.6 ml/min. c) Milling conditions: 1000 rpm, ball size 0.5 mm, ball fill level 100%, recirculation flow-rate 112.6 ml/min.
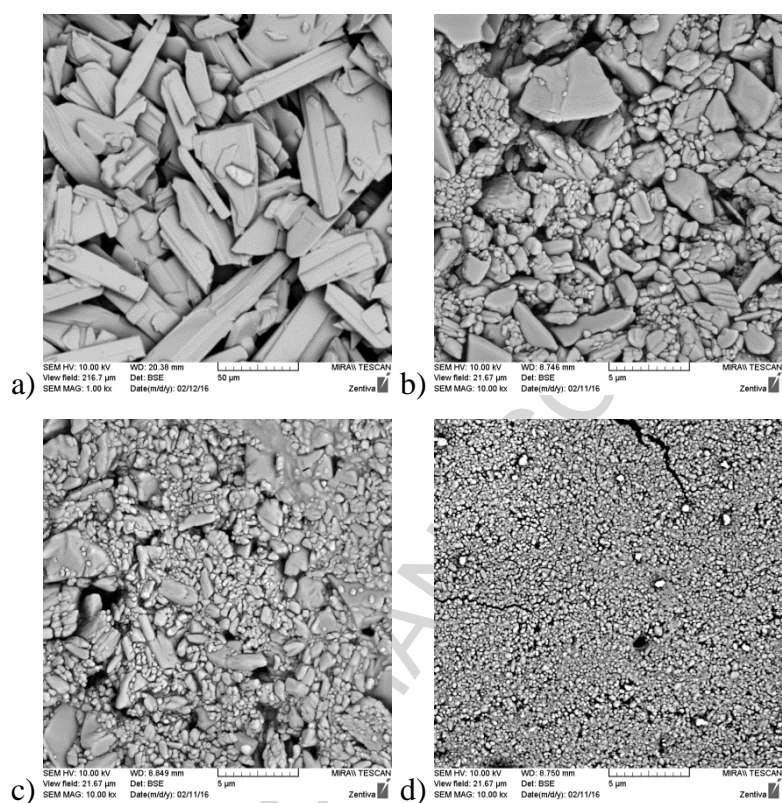
Fig. 7: SEM micrographs of samples milled under conditions from Fig. 6a. a) original raw material; b) after milling at t = 1 min; c) t = 3 min; d) t = 50 min. Note that the scale-bar represents 50 μm in case a) and 5 μm in the remaining cases.
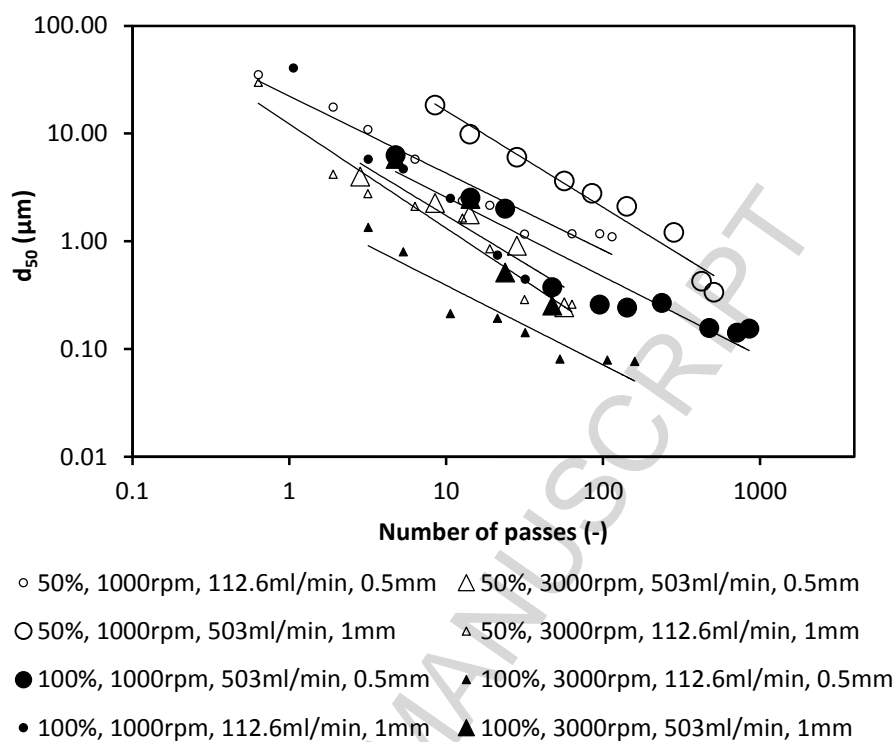
Fig. 8: Summary of the dependence of the particle size d_{50} on the number of theoretical passes through the mill (defined by Eq. 2) for all experimental conditions in a flow-through mill operated in the closed loop mode. The milling parameter values are given in the legend. The lines are regression fits by a power-law function.

Graphical abstract

32